Article

J. Mex. Chem. Soc. **2025**, *69*(3)
Regular Issue

ISSN-e 2594-0317

A Facile One-pot Four Component Synthesis of Symmetric 1,4-Dihydropyridine Derivatives using $CaFe_2O_4$ NPs as Heterogeneous Catalyst under Ultrasound Irradiation and Theoretical Studies as Potential Digestive Enzyme Inhibitors

Anjaneyulu Bendi[1,*], N. Mujafarkani[2], G. B. Dharma Rao[3,*]

[1]Department of Chemistry, Presidency University, Rajanukunte, Itgalpura, Bangalore, 560064, Karnataka, India.
[2]PG and Research Department of Chemistry/ Jamal Mohamed College (Autonomous), Affiliated to Bharathidasan University Tiruchirappalli, Tamilnadu.
[3]Department of chemistry, Kommuri Pratap Reddy Institute of Technology (Autonomous), Hyderabad-500088, India.

***Corresponding author:** Anjaneyulu Bendi, email: anjaneyulu.bendi@gmail.com; G. B. Dharma Rao, email: gbdharmarao@gmail.com

Received January 13th, 2024; Accepted September 9th, 2024.

DOI: http://dx.doi.org/10.29356/jmcs.v69i3.2193

Abstract. A fast and enormously efficient new-flanged symmetric 1,4-dihydropyridine analogs were synthesized by the one-pot four-component condensation reaction of substituted arylaldehyde, *tert*-butyl β-ketoester, $(NH_4)_2CO_3$, and benzyl alcohol with *p*-substitution via transesterification followed by Hantzsch ester synthesis using robust and recyclable $CaFe_2O_4$ NPs as heterogeneous catalyst under ultrasonic irradiation. The synthesized compounds were well characterized, and the desired derivatives were studied for the quantum chemical computations using density functional theory (DFT) with Spartan software. On the other hand, the molecular docking experience of all compounds was performed to examine their efficacy against digestive enzymes α-amylase, pepsin, and trypsin and observed that the 1,4-dihydropyridine derivatives could be used as effective digestive enzyme inhibitors.
Keywords: Hantzsch reaction; transesterification; 1,4-Dihydropyridine; ultrasound; heterogeneous catalyst; nano-particles; DFT method; molecular docking; ADMET.

Resumen. Se sintetizaron de forma rápida y altamente eficiente nuevos análogos simétricos de 1,4-dihidropiridina mediante una reacción de condensación en un solo recipiente y en cuatro componentes, utilizando arilaldehídos sustituidos, β-cetoéster tert-butilo, $(NH_4)_2CO_3$ y alcohol bencílico con sustitución en posición para a través de una transesterificación, seguida de una síntesis tipo éster de Hantzsch, empleando nanopartículas de $CaFe_2O_4$ robustas y reciclables como catalizador heterogéneo bajo irradiación ultrasónica. Los compuestos sintetizados fueron debidamente caracterizados, y los derivados obtenidos se estudiaron mediante cálculos químicos cuánticos usando la teoría del funcional de la densidad (DFT) con el software Spartan. Por otro lado, se realizó un estudio de acoplamiento molecular (docking) de todos los compuestos para evaluar su eficacia contra enzimas digestivas como α-amilasa, pepsina y tripsina, observándose que los derivados de 1,4-dihidropiridina podrían emplearse como inhibidores eficaces de enzimas digestivas.
Palabras clave: Reacción de Hantzsch; transesterificación; 1,4-dihidropiridina; ultrasonido; catalizador heterogéneo; nanopartículas; método DFT; acoplamiento molecular; ADMET.

J. Mex. Chem. Soc. **2025**, *69*(3)
Regular Issue

ISSN-e 2594-0317

Introduction

In recent years, ultrasonic irradiation transformations have acknowledged the extensive awareness by researchers and industrialists, owing to their mild reaction circumstances, moderate reaction temperature, short reaction time, and being environmentally benign. Moreover, ultrasound irradiation has become a commanding tool for a wide variety of organic transformations, and nowadays, it is commonly employed in organic reactions.[1] A chemical reaction beneath ultrasound irradiation recommends procedure-associated advantages and affords the approach for sustainable procedures.[2] Besides organic transformations, ultrasound irradiations are also found in material science, medical imaging, environmental science, molecular biology, physics, industries, and chemical engineering processes.[3-6] Ultrasonic irradiation improves the speed of various chemical transformations, such as reduction, oxidation, and polymerization procedures.[7] The principle involved in the ultrasonic technique is that ultrasonic irradiation causes deformation and bubble development, enlargement, and disintegration of micro-sized bubbles in the liquid phase. Bubble disintegrating arises across the liquid phase medium, resulting in supercritical circumstances, such as tremendous temperature (near 5000 K) and elevated pressure (near 1000 bar).[8] Deformation significantly raises the confined pressure and temperature within the deformation bubbles, producing sufficient energy for chemical derivatives and enhancing mass convey when the bubbles disintegrate.[9] Deformation engenders high-energy radical ions as reaction intermediates, which speed up the chemical reactions using the heterogeneous medium in water as a solvent, obtaining pure title products.[10] Consequently, the catalyst function might be improved beneath ultrasonic irradiation (20 to 80 kHz) transformations.

1,4-Dihydropyridine (1,4-DHP) is a fortunate moiety that was extensively considered in the past decades due to accommodating numerous promising pharmacologically and biologically active scaffolds.[11] Such a pharmacologically significant 1,4-DHP was first pioneered by Arthur Hantzsch in 1881.[12] Hence, the association of these 1,4-DHP core units in several biological developments has addressed them as a prospective therapeutic title compound of immense attention in medicinal chemistry for the reason that a broad range of pharmacological and biological properties, enormous research have been conducted throughout the last decades for the synthesis 1,4-DHP which were addressed in the literature,[13] making it an energetic and highly appropriate field of research in current days. In more than 135 years of experience with the Hantzsch reaction, most of the literature examples are restricted to three components [14], and minor structural divergences have been reported.[15]

Nanotechnology is a developing research area that deals with exclusive outstanding properties of nanoparticles.[16] The nanoparticles (NPs) have been experienced in various medical, biology, and material science applications.[17] on the other hand, a great extent of awareness was drawn to the NPs as heterogeneous catalysts. It achieved a noteworthy responsibility in organic synthesis because of its uncomplicated work-up procedure, environmentally friendly, recyclability, price effectiveness, and effortlessness of separation. Over the preceding few years, academic researchers and industrialists have been fascinated by nanoparticles as heterogeneous catalysts, which are associated with magnetic properties because of the straightforwardness of separation after the completion of the reaction using an external magnet.[18] Herein, magnetic ferrite nanoparticles afford essential magnetic behavior towards the nano-catalysts with the intention that they can be attracted by external magnets and eventually be recovered and recyclable.

Recently, Chavan et al. addressed the synthesis of pyrimidine derivatives by combining 2-amino benzimidazole, aryl aldehyde, and malononitrile using $ZnFe_2O_4$NPs under ultrasound irradiation.[19] With the support of literature precedents [20] and our previous experience in the synthesis of bio-active molecules, chemical transformations with ultrasound irradiation, and magnetic nanoparticles as heterogeneous catalysts,[21-25] there was a necessitate to synthesize a huge collection of 1,4-dihydropyridine analogs using diminish time, appreciated yields and marvelous biological activities. Herein, we have paid more attention to the ultrasound irradiation promoted four component 1,4-DHPs synthesis through the popular Hantzsch procedure using calcium Ferrite($CaFe_2O_4$) magnetic NPs as shown in Scheme 1. In addition, we also investigated the properties of the products using density functional theory (DFT), molecular docking, and ADMET for the synthesized title compounds.

J. Mex. Chem. Soc. **2025**, *69*(3)
Regular Issue

ISSN-e 2594-0317

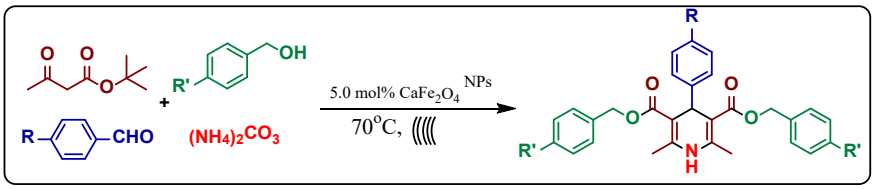

Scheme 1. 1,4-DHPs synthesis using $CaFe_2O_4$ magnetic NPs under solvent-free and ultrasound irradiation.

Experimental

All the initial precursor chemicals were acquired from Sigma-Aldrich Corporation (India) (analytical grade) and were used with no additional purification. FT-IR spectra were recorded on a Bruker IFS 55 equinox FTIR spectrophotometer through KBr discs. ^{1}H NMR and ^{13}C NMR spectra were recorded by means of Bruker 400 or 500 MHz spectrometer by TMS as internal standard. Mass analysis is analyzed on a quadruple-time of flight mass spectrometer, equipped with an esi source (+ve). TLC analysis of reaction mixtures was conducted on Merck aluminum plates (India) coated with silica gel (60 F254).

General procedure for the synthesis of symmetric 1,4-DHPs:

tert-Butyl-β-ketoester (2.0 mmol) and benzyl alcohol with para substitution (2.0 mmol) were charged in an R.B. flask and stirred at 70 °C under ultrasound irradiation for 10 min for transesterification transformation.[28] Arylaldehyde with substitution (1.0 mmol) and $(NH_4)_2CO_3$ (1.0 mmol) were further added to the above reaction mixture consequently. The reactants were combined collectively and permitted to mechanical stirring for time, as mentioned in Table 1, under ultrasound irradiation, plow the completed reaction. The improvement of reaction was observed by thin layer chromatography (TLC). After completion of the reaction, the reaction temperature was reduced to R.T. The solid mass was poured into crushed ice, filtered, and dried out using vacuum conditions. The produced mass was washed with diethyl ether, and an 82 % – 94 % yield was observed. The title product's purity was verified using spectroscopy techniques like ^{1}H-NMR and ^{13}C-NMR.

With the support from the addressed literature, a probable reaction mechanism for constructing symmetric 1,4-DHPs derivative is described in Scheme 2. At first, *tert*-butyl β-ketoester (**1**) undergoes transesterification using acetyl ketene intermediate (**2**) [29] to form a new β-ketoester (**4**) with corresponding alcohol (**3**). The new β-ketoester experiences a reaction with arylaldehyde (**5**) to form an intermediate (**6**) through Knoevenagel condensation. The Knoevenagel condensation intermediate reacts with α, β unsaturated amine ester (enamine ester, **8**), which was attained by the reaction between **4** and **7** along with dehydration to form an adduct acyclic compound (**9**). Intramolecular cyclization followed by dehydration occurs during the formation of the title Hantzsch symmetric 1,4-DHPs ester analog (**10**).

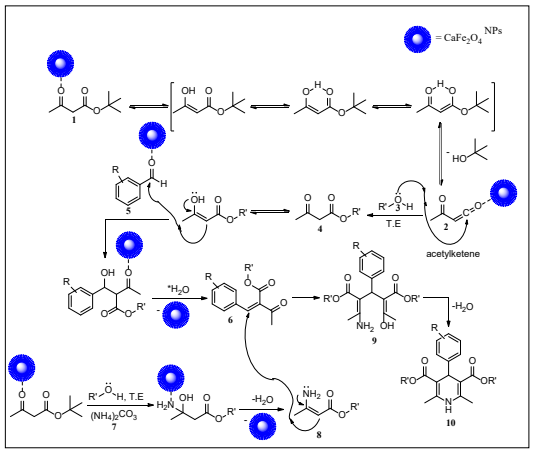

Scheme 2. Proposed mechanism for the formation of symmetrical 1,4-DHPs using $CaFe_2O_4$ NPs.

J. Mex. Chem. Soc. **2025**, *69*(3)
Regular Issue

ISSN-e 2594-0317

Computational studies

DFT studies

The DFT studies of all the 1, 4-dihydropyridine derivatives have been performed through Spartan-14 Software using the B3LYP/6-31G basis set. [30]

Geometry optimization

Table 1 indicates the optimized structure details of whole 1,4- dihydropyridine analogs performed using B3LYP/6-31G within the framework of Spartan software.

Table 1. Energies of 1,4 –dihydropyridine derivatives.

Entry	Energy (au)	E_{HOMO}	E_{LUMO}	Energy Gap	Solvation Energy (KJ/Mol)	Dipole Moment (Debye)	Polarizability
5a	-1477.01	-5.51	-1.27	4.24	-33.22	0.89	79.49
5b	-1820.59	-5.40	-1.17	4.23	-52.60	4.07	86.09
5c	-2510.73	-5.59	-1.34	4.25	-37.16	5.43	83.92
5d	-2855.81	-5.80	-1.58	4.22	-32.25	4.49	82.83
5e	-2043.10	-5.64	-1.42	4.22	-38.61	6.64	86.50
5f	-1859.90	-5.37	-1.16	4.21	-53.68	1.51	87.60
5g	-2165.66	-5.59	-1.36	4.23	-46.31	5.87	85.01
5h	-1745.38	-5.42	-1.20	4.22	-45.93	3.48	85.38
5i	-1910.57	-5.77	-2.13	3.64	-47.43	8.04	85.78
5j	-2600.71	-5.97	-2.31	3.66	-36.95	8.17	83.59

Fig. 1 represents the HOMO-LUMO energy gap of all the 1,4 –dihydropyridine derivatives, and it was observed that the derivatives **5a -5h** nearly have a similar energy gap.

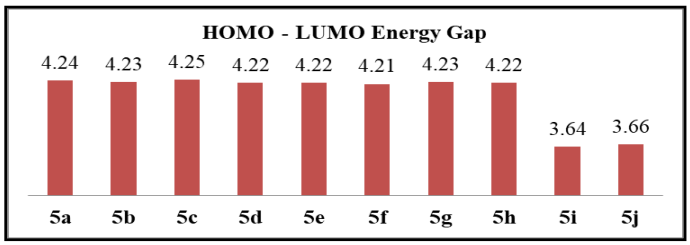

Fig. 1. HOMO – LUMO Energy Gap.

The **compound 5a** molecular geometry, electrostatic charges, mullikan charges, and natural charges have been represented in Fig. 2 and the details of the remaining derivatives are provided as supplementary material.

J. Mex. Chem. Soc. **2025**, *69*(3)
Regular Issue

ISSN-e 2594-0317

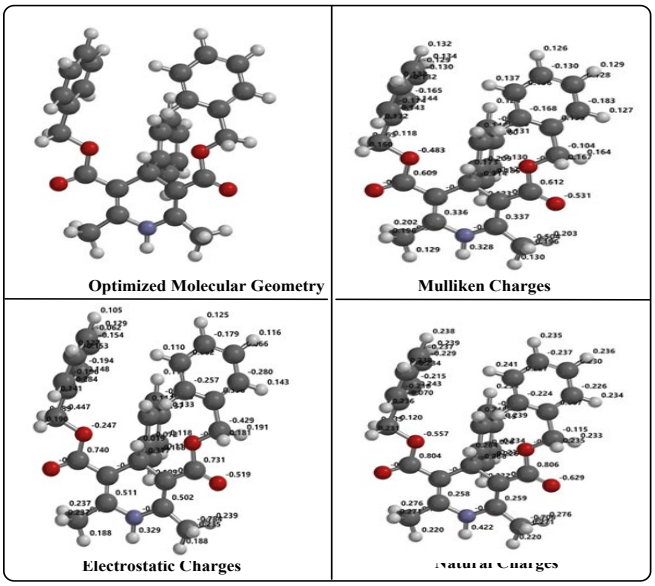

Fig. 2. Geometry Details of Compound **5a**.

Frontier Molecular Orbitals (FMO's)

FMOs offer different electrical and optical properties of the chemical compounds and their stability [31]. The FMO calculations for all the 1,4-dihydropyridine derivatives have been performed with a DFT/B3LYP/6-31G basis set. Fig. 3 depicts the HOMO and LUMO details of **compound 5a**.

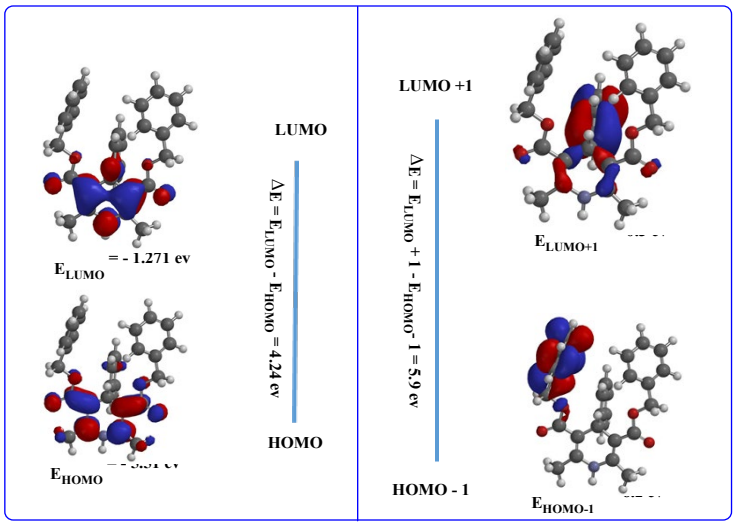

Fig. 3. FMOs of Compound **5a.**

Global reactivity descriptors

The relative stability and reactivity of 1,4- dihydropyridine derivatives have been determined by predicting their global reactivity descriptors using DFT/B3LYP/6-31G basis set through Spartan software. The highest value of each compound has been highlighted in Table 2.

J. Mex. Chem. Soc. **2025**, *69*(3)
Regular Issue

ISSN-e 2594-0317

Table 2. Global reactivity descriptors of 1,4- dihydropyridines.

Entry	IE	EA	η	μ	*S*	χ	ω	ΔNmax.	ΔEback-donation
5a	5.51	1.27	2.12	-3.39	0.47	3.39	2.71	1.60	-0.530
5b	5.40	1.17	2.12	-3.29	0.47	3.29	2.55	1.55	-0.529
5c	5.59	1.34	2.13	-3.47	0.47	3.47	2.82	1.63	-0.531
5d	5.80	1.58	2.11	-3.69	0.47	3.69	3.23	1.75	-0.528
5e	5.64	1.42	2.11	-3.53	0.47	3.53	2.95	1.67	-0.528
5f	5.37	1.16	2.11	-3.27	0.48	3.27	2.53	1.55	-0.526
5g	5.59	1.36	2.12	-3.48	0.47	3.48	2.85	1.64	-0.529
5h	5.42	1.20	2.11	-3.31	0.47	3.31	2.60	1.57	-0.528
5i	5.77	2.13	1.82	-3.95	0.55	3.95	4.29	2.17	-0.455
5j	5.97	2.31	1.83	-4.14	0.55	4.14	4.68	2.26	-0.458

Molecular Electrostatic Potential Maps (MEPs)

MEPs are helpful in the identification of reactive sites in chemical systems [32]. The MEPs of all 1, 4- dihydropyridine derivatives were computed using a DFT/B3LYP/6-31G basis set. Fig. 4 represents the MEP of **compound 5a**. The MEP data of the remaining compounds in the series have been supplied as supplementary material.

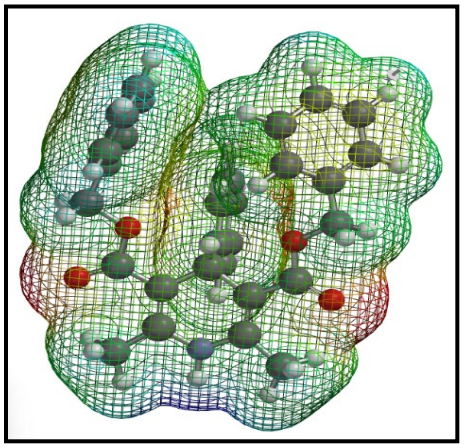

Fig. 4. MEP of Compound **5a.**

Molecular docking studies

Nowadays, molecular docking studies are playing a significant role in predicting the biological activities of organic molecules [33,34]. The efficacy of all the 1,4 –dihydropyridine derivatives has been assessed against α-amylase (PDB:1SMD) [35], pepsin (PDB:1YX9) [36], and trypsin (PDB:1AVW) [37] through Discovery Studio and Auto Dock Vina software[38]. The binding affinities of all the compounds

J. Mex. Chem. Soc. **2025**, *69*(3)
Regular Issue

ISSN-e 2594-0317

confirmed that these derivatives could act as potential inhibitors. Table 3 provides the binding energies of all the derivatives with different proteins.

Table 3. Docking studies results.

S.No.	Ligand	Binding Affinity (Kcal/mol)		
		1SMD	1YX9	1AVW
1	**5a**	-7.6	-7.5	-7.8
2	**5b**	-7.5	-7.4	-6.6
3	**5c**	-7.8	-7.8	-7.7
4	**5d**	-8.0	-7.8	-6.6
5	**5e**	-8.1	-8.9	-7.2
6	**5f**	-7.3	-8.3	-7.5
7	**5g**	-7.7	-7.1	-6.7
8	**5h**	-7.7	-7.3	-6.6
9	**5i**	-7.6	-8.2	-6.7
10	**5j**	-7.5	-8.0	-8.6

The **compound 5e** has shown the highest binding energy of -8.1 k.cal/mol with α-amylase based protein (PDB:1SMD), and the corresponding interactions have been represented in Fig. 5. The binding energy range has been observed between -7.3 to -8.1 k.cal/mol. The docking studies data of other compounds are given as supplementary material.

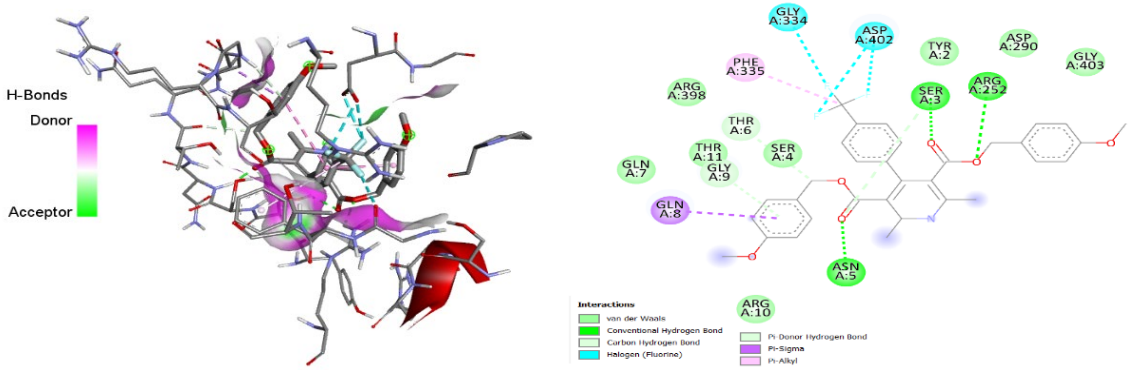

Fig. 5. Compound 5e interactions with 1SMD Protein.

The **compound 5e** has shown the highest binding energy of -8.9 k.cal/mol with pepsin based protein (PDB:1YX9), and the corresponding interactions have been represented in Fig. 6. The binding energy range

J. Mex. Chem. Soc. **2025**, *69*(3)
Regular Issue

ISSN-e 2594-0317

has been observed between -7.1 to -8.1 kcal/mol. The supporting information has supplied the docking studies data of the remaining compounds in the series.

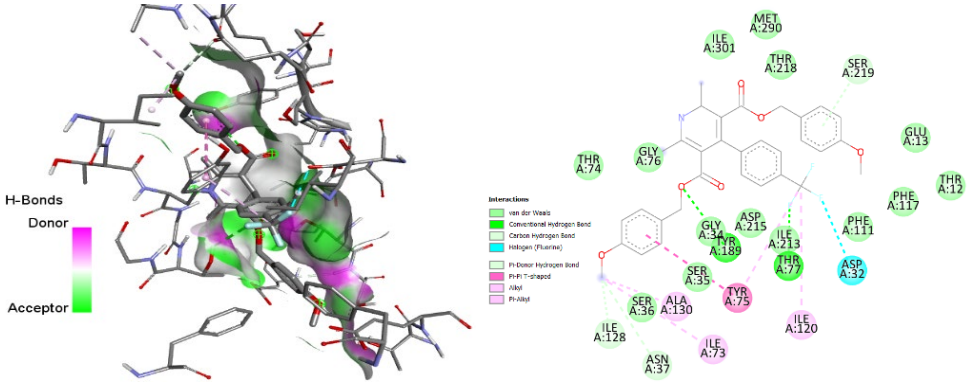

Fig. 6. Compound 5e interactions with 1YX9 protein.

The **compound 5j** has shown the highest binding energy of -8.6 k.cal/mol with trypsin based protein (PDB:1AVW), and the corresponding interactions have been represented in Fig. 7. The binding energy range has been observed between -6.6 to -8.1 k.cal/mol. The docking studies data of the remaining compounds in the series have been supplied in the supporting information.

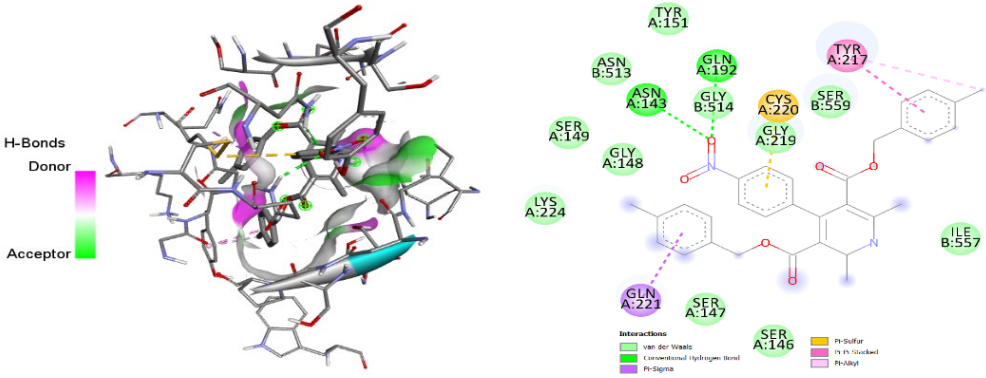

Fig. 7. Compound 5j interactions with 1AVW protein.

ADMET properties

1,4 –dihydropyridine derivatives drug-likeness properties have been evaluated using the Swiss ADME web tool [39], and the results related to its drug-likeness and bioavailability have been given in Table 4 and Table 5.

J. Mex. Chem. Soc. **2025**, *69*(3)
Regular Issue

ISSN-e 2594-0317

Table 4. Results of ADMET studies.

Entry	Formula	M.Wt (g/mol)	NRB	NHA	NHD	TPSA (A^{o2})	LogP (cLogp)	Lipinski's Rule Violations	Synthetic Accessibility
5a	$C_{29}H_{27}NO_4$	453.53	9	4	1	64.63	4.78	Yes	4.50
5b	$C_{32}H_{33}NO_7$	543.61	12	7	1	92.32	4.74	Yes	4.92
5c	$C_{30}H_{27}Cl_2NO_5$	552.45	10	5	1	73.86	5.81	No	4.59
5d	$C_{29}H_{24}Cl_3NO_4$	556.86	9	4	1	64.63	6.21	No	4.48
5e	$C_{32}H_{30}F_3NO_6$	581.58	12	9	1	83.09	5.83	No	4.90
5f	$C_{33}H_{35}NO_7$	557.63	13	7	1	92.32	4.98	No	5.04
5g	$C_{31}H_{30}ClNO_6$	548.03	11	6	1	83.09	5.32	No	4.74
5h	$C_{32}H_{33}NO_6$	527.61	11	6	1	83.09	5.12	No	4.87
5i	$C_{31}H_{30}N_2O_8$	558.58	12	8	1	128.91	3.19	No	4.82
5j	$C_{29}H_{24}Cl_2N_2O_6$	567.42	10	6	1	110.45	4.98	No	4.54

TPSA=Total Polar Surface Area, NHD=Number of Hydrogen Donors, NRB=Number of Rotatable Bonds and NHA= Number of Hydrogen Acceptors

J. Mex. Chem. Soc. **2025**, *69*(3)
Regular Issue

ISSN-e 2594-0317

Table 5. Results of ADMET studies with reference to toxicity.

Entry	Skin Permeation (logKp) cm/s	GI Absorption	BBB Permiability	P-gp Sunstrate	CYP1A2 Inhibitor	CYP2C19 Inhibitor	CYP2C9 Inhibitor	CYP2D6 Inhibitor	CYP3A$ Inhibitor
5a	-5.13	High	Yes	Yes	No	Yes	Yes	No	Yes
5b	-5.75	High	No	Yes	No	Yes	Yes	Yes	Yes
5c	-4.86	High	No	Yes	No	Yes	Yes	No	Yes
5d	-4.43	High	No	Yes	No	Yes	Yes	No	Yes
5e	-5.32	Low	No	Yes	Yes	Yes	Yes	Yes	Yes
5f	-5.57	High	No	Yes	Yes	Yes	Yes	Yes	Yes
5g	-5.30	High	No	Yes	Yes	Yes	Yes	No	Yes
5h	-5.36	High	No	Yes	No	Yes	Yes	Yes	Yes
5i	-5.94	Low	No	Yes	No	Yes	Yes	No	Yes
5j	-5.05	Low	No	No	Yes	Yes	Yes	No	Yes

CYP=Cytochrome-P, GI=Gastrointestinal, P-gp=P-Glycoprotein and BBB=Blood Brain Barrier

J. Mex. Chem. Soc. **2025**, *69*(3)
Regular Issue

ISSN-e 2594-0317

Bioavailability radar and BOILED-Egg model of **Compound 5a** has been determined using **Swiss ADME software** and the relevant data shown in Fig. 8.

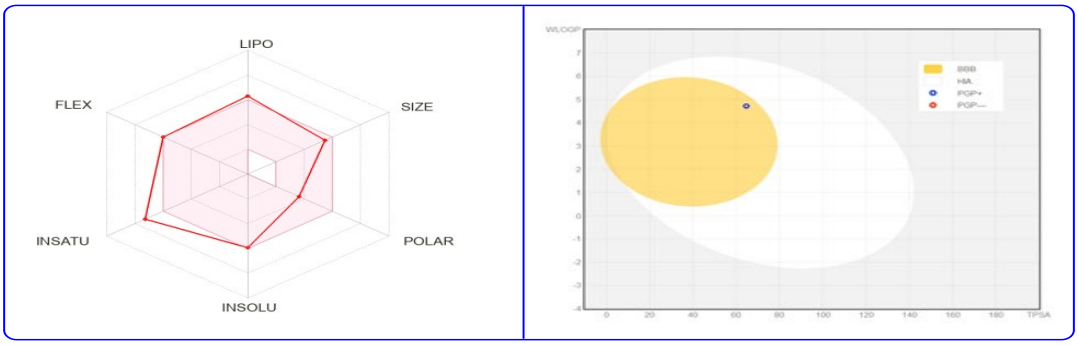

Fig. 8. (Left) Bioavailability radar and (Right) BOILED-Egg model of **Compound 5a**.

The ideal physiochemical area for oral bioavailability is the coloured zone, which contains each molecule's physiochemical characteristics and indicates its oral activity.

Server molinspiration [40] was utilized in addition to their drug-like properties to determine the bioactivity score of the analogues against various receptors, such as nuclear receptor, GPCR (G-protein coupled receptor), ion channel, kinase, and protease, in order to compare and assess the likelihood that they are active compounds as described in Table 6.

Table 6. Drug-likeness properties for the synthesized compounds using molinspiration software.

Entry	GPCR Ligand	Ion Channel Modulator	Kinase Inhibitor	Nuclear Receptor Ligand	Protease Inhibitor	Enzyme Inhibitor
5a	-0.15	-0.01	-0.58	-0.10	-0.31	-0.23
5b	-0.16	-0.27	-0.57	-0.16	-0.31	-0.29
5c	-0.17	-0.16	-0.56	-0.12	-0.35	-0.27
5d	-0.14	-0.07	-0.55	-0.11	-0.32	-0.23
5e	-0.17	-0.38	-0.61	-0.18	-0.28	-0.38
5f	-0.22	-0.38	-0.64	-0.22	-0.34	-0.37
5g	-0.16	-0.22	-0.57	-0.14	-0.34	-0.29
5h	-0.19	-0.26	-0.58	-0.15	-0.35	-0.30
5i	-0.27	-0.39	-0.70	-0.27	-0.39	-0.41
5j	-0.24	-0.21	-0.64	-0.20	-0.41	-0.34

Results and discussion

$CaFe_2O_4$ magnetic NPs were synthesized by a straightforward co-precipitation procedure by means of sodium hydroxide as a precipitating agent. The synthesized $CaFe_2O_4$ NPs were illustrated by XRD

J. Mex. Chem. Soc. **2025**, *69*(3)
Regular Issue

ISSN-e 2594-0317

characterization at JNU, New Delhi, TEM characterization at IARI, New Delhi, Fourier-transform infrared spectroscopy, and N_2 adsorption-desorption isotherm analysis characterization at University of Delhi, New Delhi.[26]

Hence, in observance of this information in the notice, in this communication, we were paying attention to accomplishing the synthesis of 1,4-dihydropyridine analogs employing the required catalytic amount of $CaFe_2O_4$ Magnetic NPs under ultrasound irradiation. To examine the reaction circumstances, benzaldehyde, tert-butyl β-ketoester, $(NH_4)_2CO_3$and benzyl alcohol (Table 7, Entry 2) were in use as test reactants using a catalytic quantity of $CaFe_2O_4$magnetic NPs under ultrasound irradiation by via Hantzsch reaction. It was observed that, while benzaldehyde, tert-butyl β-ketoester, $(NH_4)_2CO_3$and benzyl alcohol were employed in the mole ratio of 1:2:1:2 using a catalytic quantity of $CaFe_2O_4$ magnetic NPs under ultrasound irradiation, results in corresponding 1,4-dihydropyridine analog and found as best result given reaction time and satisfactory yields.

As per the above-existing reaction deliberations, we observed the distinct catalyst mole concentrations for observing 1,4-DHP derivatives using $CaFe_2O_4$magnetic NPs as heterogeneous catalysts at 70°C. To examine the probability of the distinct catalyst mole concentrations, the test reaction is carried out with test reactants for the corresponding four components 1,4-DHP (Table 7, Entry 2) and set the constant reaction time to 30 min under ultrasound irradiation. 80 %, 83 %, 85 %, 89 %, and 92 % yields were obtained using 1.0, 2.0, 3.0, 4.0 and 5.0 mol% of $CaFe_2O_4$magnetic NPs respectively. On the other hand, a 78 % yield was observed under the catalyst-free condition. Nevertheless, among every catalytic concentration, it was found that 5.0 mol% of $CaFe_2O_4$magnetic NPs (Fig. 9 bar 6) was established to be the most valuable for the Hantzsch chemical transformation, as shown in Fig. 1. On the other hand, it was also noticed that a boost in the quantity of catalyst (6.0 mol% and 7.0 mol%) did not improve the % yield of 1,4-DHP.

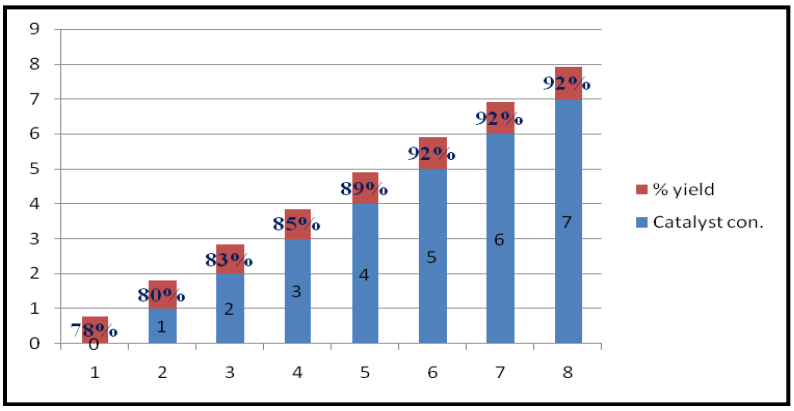

Fig. 9. Effect of $CaFe_2O_4$ magnetic NPs concentration for the synthesis of 1,4-DHP under ultrasonic irradiation.

Throughout investigative reactions, we also examined the four component condensation reaction of test reactants benzaldehyde, *tert*-butyl β-ketoester, $(NH_4)_2CO_3$ and benzyl alcohol (Table 7, Entry 2) in the mole ratio of 1:2:1:2 under ultrasound irradiation for 30 min as reaction time using different magnetic property catalysts and obtained the 92 %, 81 % and 74 % yields using $CaFe_2O_4$ nano-particles, $CoFe_2O_4/Cu(OH)_2$ nanocomposite, $CuFe_2O_4$ nano-particles correspondingly. Moreover, the reaction was studied under catalyst-free circumstances; the preferred product was formed with a modest yield of 78 %, even though $CaFe_2O_4$NPs effectively experienced the reaction and obtained the elevated yield of the particular 1,4-DHP product (Table 7, Entry 2) beneath no solvent and ultrasound irradiation.

J. Mex. Chem. Soc. **2025**, *69*(3)
Regular Issue

ISSN-e 2594-0317

Table 7. $CaFe_2O_4$ magnetic NPs catalyzed synthesis of 1,4-DHPs analogues beneath ultrasound irradiation and no solvent circumstances.[a,b]

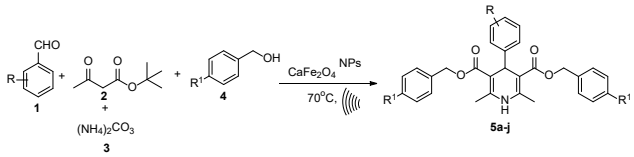

S.No.	R	R^1	Time (min.) for method-A	Product[a]	(%) yield[b]		m.p (°C)[ref]
					method-A	method-B (2.5 h)	
1	4-H	4-H	30	**5a**	92 %	83 %	116-118
2	4-OCH_3	4-OCH_3	30	**5b**	92 %	90 %	128-130[19]
3	4-OCH_3	4-Cl	35	**5c**	94 %	92 %	124-126[19]
4	4-Cl	4-Cl	40	**5d**	84 %	82 %	132-134
5	4-CF_3	4-OCH_3	40	**5e**	92 %	89 %	142-144[19]
6	4-OC_2H_5	4-OCH_3	30	**5f**	92 %	78 %	100-102[19]
7	4-Cl	4-OCH_3	35	**5g**	86 %	83 %	150-152[19]
8	4-CH_3	4-OCH_3	30	**5h**	94 %	94 %	98-100[19]
9	4-NO_2	4-OCH_3	40	**5i**	82 %	75 %	178-180[19]
10	4-NO_2	4-Cl	45	**5j**	87 %	78 %	154-156[19]

[a]Reaction conditions: Substituted benzaldehyde (1.0 mmol), *tert*-butyl β-ketoester (2.0 mmol) $(NH_4)_2CO_3$ (1.0 mmol) and 4-substituted benzylalcohol (2.0 mmol) at 70 °C using 5.0 mol% $CaFe_2O_4$.
[b]Isolated Yields

The feasibility of these standardized reaction circumstances and substrate extent of this procedure has also been expanded to various substituted benzaldehydes and benzyl alcohols. The procedure shows the capability of both EWD and ED groups on benzaldehyde. It is available in diverse benzyl alcohol to offer the equivalent predictable 1,4-dihydropyridine with excellent to satisfactory yields. All the outcomes were tabulated in Table 7. The novel, highly developed procedure (Method-A) is furthermore evaluated through the previously addressed procedure (Method-B).[27] The latest four-component one-pot Hantzsch reaction in the direction of the production of 1,4-dihydropyridine is recommended additional advantages compared with formerly addressed conventional reactions in provisions of diminished reaction time, easygoing reaction circumstances, atom economy, and price-effectiveness. The purity of synthesized compounds is verified by authentic compounds [19], the newly (**5d**) synthesized derivatives are characterized, and the spectral data is shown below.

Spectral characterization

Dibenzyl 2,6-dimethyl-4-phenyl-1,4-dihydropyridine-3,5-dicarboxylate (5a): Physical State: White solid; **yield**: 92 %. **mp** 116–118 °C. **FTIR (KBr, ν/cm)** 3342, 3204, 1947, 1692, 1542, 1456, 1297, 808, 770, 735. **^{1}H NMR (400 MHz, $CDCl_3$)** δ 7.26 (–C_6H_5, d, J = 2.8 Hz, 2H), 7.24–7.20 (–C_6H_5, m, 5H), 7.08–7.03 (– C_6H_5, m, 5H), 6.68–6.64 (–C_6H_5, d, J = 8.6 Hz, 3H), 5.68 (-NH, s, 1H), 5.12–5.08 (-OCH_2Ph, d, J = 12.7 Hz, 2H), 4.96–4.92 (-OCH_2Ph, –C_6H_5, m, 3H), 2.27 (–CH_3, s, 6H). **^{13}C NMR (100 MHz, $CDCl_3$)** δ 167.12, 158.10, 144.25, 139.88, 135.1, 133.66, 129.33, 129.28, 129.04, 128.54, 128.51, 113.28, 104.1, 64.76, 38.68, 19.68. **ESI–MS:** m/z 453.19 $[M + 1]^+$. **Anal. Cal. for $C_{29}H_{27}NO_4$**: C, 76.8; H, 6.0; N, 3.09. Found: C, 76.6; H, 6.1; N, 3.1.

J. Mex. Chem. Soc. **2025**, *69*(3)
Regular Issue

ISSN-e 2594-0317

Bis(4-chlorobenzyl) 4-(4-chlorophenyl)-2,6-dimethyl-1,4-dihydropyridine-3,5-dicarboxylate (5d): **Physical State:** White solid; **yield**: 84 %. **mp** 132–134 °C. **FTIR (KBr, ν/cm)**: 3338, 3149, 1950, 1682, 1545, 1488, 1305, 802, 770, 738. **^{1}H NMR (400 MHz, $CDCl_3$)** δ 7.34 (–C_6H_5, d, J = 2.8 Hz, 2H), 7.22–7.19 (–C_6H_5, s, 2H), 7.10–7.03 (– C_6H_5, m, 5H), 6.68–6.64 (–C_6H_5, d, J = 8.6 Hz, 3H), 5.70 (-NH, s, 1H), 5.10–5.04 (-OCH_2Ph, d, J = 12.8 Hz, 2H), 4.94–4.87 (-OCH_2Ph, –C_6H_5, m, 3H), 2.32 (–CH_3, s, 6H). **^{13}C NMR (100 MHz, $CDCl_3$)** δ 168.14, 159.08, 145.24, 138.90, 136.07, 132.64, 128.37, 128.30, 128.02, 127.61, 127.52, 112.31, 105.07, 63.78, 37.76, 19.81. **ESI–MS:** m/z 556.1 $[M + 1]^+$. **Anal. Cal. for $C_{29}H_{24}Cl_3NO_4$**: C, 62.55; H, 4.34; Cl, 19.10; N, 2.52. Found: C, 62.54; H, 4.34; Cl, 19.12; N, 2.54.

Recyclability of $CaFe_2O_4$ magnetic NPs

From a green chemistry and sustainability point of examination, efficient revitalization and recycling of the catalyst is extremely attractive. As a result, the revitalization and reusability of $CaFe_2O_4$magnetic NPs were examined using solvent-free and ultrasonic irradiation. The catalyst can be recollected with an external magnet after the reaction from the R.B. flask and washed with hot ethanol. The catalyst was reprocessed in a similar process for consecutive runs (capable of 03 sequences) beneath similar reaction circumstances; the variation in catalytic capability was also examined in observations of (%) yield. We confirmed that the corresponding 1,4-dihydropyridine (Table 7, Entry 2) attained satisfactory % yields without suffering any catalytic activity, as shown in Fig. 10.

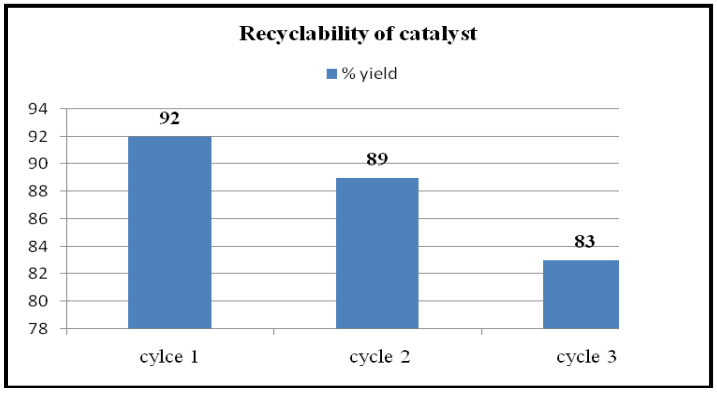

Fig. 10. Recyclability of $CaFe_2O_4$ magnetic.

Conclusions

In conclusion, we have expressed an uncomplicated and proficient one-pot four-component process in synthesizing symmetric 1,4-dihydropyridine analogs with $CaFe_2O_4$ magnetic nanoparticles as an effective heterogeneous catalyst using ultrasound irradiation without the usage of any solvent. The remarkable virtues of this procedure are the simple operation, easygoing reaction circumstances, effortlessness of the work-up process, and exceptional recyclability of the magnetic NPs catalyst. $CaFe_2O_4$ magnetic NPs make the reaction inexpensive, making the process attractive to the offered procedures in literature for observing 1,4-DHP analogs. We presume with the intention of the existing protocol furnished the desired target molecules in outstanding to satisfactory yields at diminished reaction time, which might be owing to the enhanced reactivity of the precursors on the high surface area of $CaFe_2O_4$ magnetic nanoparticles. The theoretical DFT and molecular docking studies confirmed that these compounds can be used as potential inhibitors against α-amylase, pepsin, and trypsin digestive enzymes. This manuscript provides a pathway for young researchers to explore the chemistry of 1,4-dihydropyridine analogs as potential digestive enzyme inhibitors.

J. Mex. Chem. Soc. **2025**, *69*(3)
Regular Issue

ISSN-e 2594-0317

Acknowledgments

Authors wish to truly thank the management of Presidency University, Bangalore, Karnataka, Jamal Mohamed College (Autonomous), Tiruchirappalli, Tamilnadu, and KPRIT (Autonomous), Ghatkesar, Hyderabad, Telangana for the constant support to conduct the research work and submit for publication.

References

1. Saranya, S.; Radhika, S.; Abdulla, C. M. A.; Anilkumar, G. *J. Heterocyclic Chem.* **2021**, *1*-11.
2. Draye, M.; Chatel, G.; Duwald, R. *Pharmaceuticals*. **2020**, *13*, 1-35.
3. Chandan, R.; Mehta, S.; Banerjee, R. *Biomater. Sci. Eng.* **2020**, *6*, 4731–4747.
4. Deng, Q.; Mi, J.; Dong, J.; Chen, Y.; Chen, L.; He, J.; Zhou, J. *ACS Nano*, **2023**, *17*, 263-274.
5. Debnath, K.; Sarkar, A. K.; Jana, N. R.; Jana, N. R. *Acc. Mater. Res.* **2022**, *3*, 54-66.
6. Kashkooli, F. M.; Jakhmola, A.; Hornsby, T. K.; Tavakkoli, J.; Kolios, M. C. *J. Control. Release*. **2023**, *355*, 552-578.
7. Weissler, A. *J. Acoust. Soc. Am.* **1953**, *25*, 651–657.
8. Rad, T. S.; Ansarian, Z.; Khataee, A.; Vahid, B.; Doustkhah, E. *Sep. Purif. Technol.* **2021**, *256*, 117811.
9. Cella, R.; Stefani, H. A. *Tetrahedron*. **2009**, *65*, 2619–2641.
10. Stefani, H. A.; Cella, R., in: *Encyclopedia of Physical Organic Chemistry*; John Wiley & Sons, **2017**, 1–25.
11. Saini, K. K.; Rani, R.; Muskan; Khanna, N.; Mehta, B.; Kumar, R. *Curr. Org. Chem.* **2023**, *27*, 119-129.
12. Hantzsch, A. *Chem. Ber.* **1881**, *14*, 1637-1638.
13. Sohal, H. S. *Mater. Today: Proc.* **2022**, *48*, 1163-1170.
14. Dharma Rao, G. B.; Nagakalyan, S.; Prasad, G. K. *RSC Adv.* **2017**, *7*, 3611-3616.
15. Jadeja, K. F.; Joshi, H. S. *Anal. Chem. Lett.* **2022**, *12*, 371-379.
16. Xia, Y. N.; Yang, P. D.; Sun, Y. G.; Wu, Y. Y.; Mayers, B.; Gates, B.; Yin, Y. D.; Kin, F.; Yan, H. Q. *Adv. Mater.* **2003**, *15*, 353.
17. Chan, S. S.; Low, S. S.; Chew, K. W.; Ling, T. C.; Rinklebe, J.; Juan, J. C.; Ng, E. P.; Show, P. L. *Environ. Res.* **2022**, *212*, 113140.
18. Chandel, M.; Ghosh, B. K.; Moitra, D.; Patra, M. K.; Vadera, S. R.; Ghosh, N. N. *J. Nanosci. Nanotechnol.* **2018**, *18*, 2481-2492.
19. Chavan, P.; Bangale, S.; Pansare, D.; Shelke, R.; Jadhav, S.; Tupare, S.; Kamble, D.; Rai, M. *J. Heterocyclic Chem.* **2020**, *1*-8.
20. Shearer, C.; Desaunay, O.; Zorc, S.; Richaud, A. D.; Samanta, S. S.; Jeedimalla, N.; Roche, S. P. *Tetrahedron*. **2019**, *75*, 130606.
21. Anjaneyulu, B.; Dharma Rao, G. B.; Sharma, N.; Singh, M. P. *Results Chem.* **2021**, *3*, 100202.
22. Anjaneyulu, B.; Dharma Rao, G. B.; Bajaj, T. *Results Chem.* **2021**, 100093.
23. Anjaneyulu, B.; Dharma Rao, G. B.; Nancy; Nagakalyan, S. *J. Saudi Chem. Soc.* **2021**, *25*, 101394.
24. Anjaneyulu, B.; Dharma Rao, G. B.; Sharma, N.; Tomar, R.; Singh, L. *ChemistrySelect*. **2022**, *7*, e202103910, 1-10.
25. Anjaneyulu, B.; Dharma, G. B. *Lett. Org. Chem.* **2023**, *20*, 568-578.
26. Anjaneyulu, B.; Arti, S.; Dharma Rao, G. B.; Raza, M. J.; Sharma, N. *J. Chem.* **2021**, 1-12.
27. Dharma Rao, G. B. *J. Heterocyclic Chem.* **2018**, *55*, 2556-2562.
28. Dharma Rao, G. B.; Kaushik, M. P. *Tetrahedron Lett.* **2011**, *52*, 5104-5106.
29. Witzeman, J. S.; Nottingham, W. D. *J. Org. Chem.* **1991**, *56*, 1713.
30. Spartan'14, 2014, Wavefunction Inc., Irvine.
31. Fleming, I., in: *Frontier Orbitals and Organic Chemical Reactions*, Wiley, London, **1976**.
32. Okulik, N.; Jubert, A. H. *J. Mol. Struct.* **2004**, *682*, 55–62.

J. Mex. Chem. Soc. **2025**, *69*(3)
Regular Issue

ISSN-e 2594-0317

33. Agu, P. C.; Afiukwa, C.A.; Orji, O.U.; Ezeh, E. M.; Ofoke, I. H.; Ogbu, C. O.; Ugwuja, E. I.; Aja, P. M. *Sci. Rep.* **2023**, *13*, 13398.
34. Meng, X. Y.; Zhang, H. X.; Mezei, M.; Cui, M. *Curr. Comput.-Aided Drug Des.* **2011**, *7*, 146-157.
35. Ramasubbu, N.; Paloth, V.; Luo, Y.; Brayer, G. D.; Levine, M. J. *Acta Cryst.* **1996**, *D52*, 435-446.
36. Kesavulu, M. M.; Ramasubramanian, S.; Suguna, K. *Biochem. Biophys. Res. Commun.* **2005**, *331*, 1510-1514.
37. Song, H. K.; Suh, S. W. *J. Mol. Biol.* **1998**, *275*, 347-363.
38. Trott, O.; Olson, A. J. *J. Comput. Chem.* **2010**, *31*, 455-461.
39. Daina, A.; Michielin, O.; Zoete, V. *Sci. Rep.* **2017**, *7*, 42717.
40. Molinspiration. (n.d.). Molinspiration: Computational chemistry tools for drug discovery.